Tahir Rasheed
IRT Jules Verne,
1 Mail des 20 000 Lieues 44340,
Nantes, FRANCE
email: tahir.rasheed@irt-jules-verne.fr

Loic Michel
LS2N, UMR CNRS 6004,
Centrale Nantes, FRANCE
email: loic.michel@ec-nantes.fr

Stéphane Caro
LS2N, UMR CNRS 6004,
CNRS, FRANCE
email: stephane.caro@ls2n.fr

Jean-Pierre Barbot
QUARTZ EA 7393, ENSEA,
Cergy-Pontoise, France
LS2N, UMR CNRS 6004,
Centrale Nantes, FRANCE
email: barbot@ensea.fr

Yannick Aoustin[1]
LS2N, UMR CNRS 6004,
Nantes Université, FRANCE
email: yannick.aoustin@univ-nantes.fr

Dynamic Parameter Identification for Cable-Driven Parallel Robots

This paper presents an initial work of identifying the dynamic parameters for cable-driven parallel robot (CDPR), CRAFT with a rigorous protocol. An orbital trajectory of the platform is designed in order to get a pure translation movement of the platform. This trajectory evolves in a plane and allows the identification of four dynamic parameters, the mass of the platform and the first three moments along the three main axes. From experimental data obtained with the moving-platform, the linear velocity and acceleration of the platform, which are necessary for parameters identification of the CDPR, are calculated with the application of an algorithm using semi-implicit homogeneous differentiators. The obtained identification results show that in spite of the complexity of CRAFT an identification of all its essential dynamic parameters is possible. Moreover, in the long term, an online identification of CRAFT during handling tasks is envisaged.

Keywords: Cable-Driven Parallel Robots, Inverse Dynamic Model, Dynamic Parameter Identification, Least-squares estimator, Semi-Implicit Euler Homogeneous Differentiator, Experiments

1 Introduction

The objective is to initiate a scientific approach in order to identify the essential dynamic parameters of a cable-driven parallel robot (CDPR). A CDPR consists of a moving-platform (MP) that is connected to a rigid frame by means of cables and actuators, the latter being generally mounted on the ground. These robots are very attractive for handling tasks [1] because of their low inertia, a higher payload to weight ratio and a large workspace compared to conventional manipulator robots with articulated rigid limbs. Their possible application fields can be industrial, or dedicated to search-and-rescue operations. To deal with various restrictions on cable tensions, cable elasticity, collisions and obstacle avoidance, over-actuation of the MP is actually a challenging scientific problem [2], [3].

The control of a CDPR is complex because, among other things, whatever its movement, the tension of its cables must always be positive. There are still open problems in the control of CDPRs. One key example of an open problem is that control design requires a consistent dynamic model with a relatively good knowledge of the dynamic parameters of the robot such as the terms of inertia, mass, and even friction at the actuator level, which manage the winding of the cables. Several contributions about identification of a robot cable exist. Kraus *et al.* [4] present an identification method for the complete actuator of a cable robot. A second-order system is established with a dead time as an analogous model. An inverse dynamic method (IDM) is used to identify the model parameters of a cable-driven finger joint for surgical robot [5]. But to our best knowledge the identification parameters of the handling platform of a cable robot during a movement in space is not currently investigated.

A CDPR, named *CRAFT* and located at LS2N, Centrale Nantes campus, is equipped with eight actuators and a MP. Each motor has an encoder sensor measuring the angular velocity of its output shaft allowing to evaluate the performances of the differentiation solutions. The MP has six degrees of freedom (DoF). This MP is thus over-actuated [6].

The identification of the dynamic parameters of a robot is essential to evaluate its behavior in simulation or to synthesize a control based model. The objective of the identification is not to find physical parameters of a mechanism as a robot, whose value is the most exact possible but to provide a modeling tool that is consistent in order to make simulation, control or other. The identification methodology is usually based on an inverse dynamic model that is linear as a function of the dynamic parameters to be identified [7], [8], or [9]. Any matrix inversion, which is generally a generator of numerical problems, is thus avoided. However the identification of dynamic parameters is not easy when the dynamic model is complex. Among the many challenges to be met is the search for exciting trajectories to identify the greatest number of dynamic parameters and overcome noise problems [10]. However the identification of dynamic parameters is not easy when the dynamic model is complex. The dynamic behavior of the *CRAFT* that moves in 3D space with rotation and translation combinations effectively requires a complex modeling with a lot of inertial parameters. In addition, one or more cables may slacken unexpectedly. As a consequence to initiate an identification work, only the model of the platform maneuvered by the cables is considered. Moreover, the defined trajectories generate only translation movements of the platform, *i.e.* without any rotational movement of the platform with respect to itself, in a plane. The model to describe the dynamic behavior of *CRAFT* becomes simpler with only four dynamic parameters to identify. To manage the noise problems semi-implicit Euler homogeneous differentiators are proposed (see e.g. [11] for a comparison of the techniques) and [12]. Off-line identification was conducted in order to compare, respectively from the planned trajectories of the platform, the measured filtered signals and their simplest Euler differentiation, and measured signals

[1]Corresponding Author.
February 10, 2025

processed with an original semi-implicit homogeneous differentiators without extra filter. The main advantage of the semi-implicit Euler homogeneous differentiators is to offer the perspective of a real-time identification of dynamic parameters of *CRAFT*.

The contribution of this work is based on three parts: Elaboration of a protocol in order to work with a dynamic model for translational movements of the platform and to have only four parameters to identify and experimental definition of this movement; Identification of the four parameters starting respectively from the reference trajectory, the tension measurement of the cable tension, the position measurement and the application of the simplest Euler differentiation to obtain the linear velocity and acceleration signals. Furthermore these velocity and acceleration signals are compared with those obtained an original semi-implicit Euler homogeneous differentiator. The long-term idea of this work is to develop a complete framework that brings together numerical identification and derivation tools to identify the dynamic parameters of the on-line *CRAFT* as it performs handling tasks.

The remaining of the paper is outlined as follows. Section 3 is devoted to the presentation of *CRAFT* namely, its geometric, kinematic, dynamic model and its adaptation to the presented strategy. The identification methodology, which is based on the least-squares (*LS*) estimator is presented in Sec. 4, with the solving way. A semi-implicit homogeneous differentiator, which is considered in this study to get the velocities and the accelerations from the measured position, is presented Sec. 6. The experimental results are presented in Sec. 7. Conclusions and future work are offered in Sec. 8.

2 Robot *CRAFT*

The cable-driven parallel robot prototype, named *CRAFT* is located at LS2N, France. The base frame of *CRAFT* is 4 m long, 3.5 m wide, and 2.7 m high, see Figure 1). The three- translational and the three- rotational motions of its suspended *MP* are controlled with eight cables being respectively wound around eight actuated reels fixed to the ground. The *MP* is 0.28 m long, 0.28 m wide, and 0.2 m high, its overall mass being equal to 5 kg. For each of the eight electrical motors an encoder sensor measures the angular variable of its shaft. The eight motors are equipped with a gearbox reducer of ratio $n_r = 8$. The measured value is divided by n in order to obtain the angular position of the output shaft of the gearbox reducer. The robot *CRAFT* has no tachometer.

The main hardware of the prototype consists of a PC (equipped with © MATLAB and © ControlDesk software), eight © PARKER SME60 motors and TPD−M drivers, a © dSPACE DS1007-based real-time controller and eight custom made winches. Each cable can exert a tension up to 150 N to the *MP*. The maximum velocity of each cable is equal to 5.9 m/s. The cable tensions are measured using eight *FUTEK FSH04097* sensors, one for each cable, attached to cable anchor points. Their signal is amplified using eight FSH03863 voltage amplifiers and sent to the robot controller by a coaxial cable. *CRAFT* is equipped with a motion capture, *OptiTrack* that the sampling period is equal to 0.01 s.

3 Robot Modeling

Figure 1 depicts the main geometric parameters of *CRAFT* and the i^{th} cable where $i \in \{1, \ldots, m\}$, m being the number of cables attached to the n DoF *MP* (for *CRAFT*, $m = 8$ and $n = 6$). The dynamic equilibrium wrench equation can be expressed as:

$$\mathbf{W}\boldsymbol{\tau} - \mathbb{I}_p\ddot{\mathbf{p}} - \mathbf{C}\dot{\mathbf{p}} + \mathbf{w}_g = \mathbf{0}_m \tag{1}$$

with $\mathbf{W}$ being the robot wrench matrix expressed as:

$$\mathbf{W} = \begin{bmatrix} \mathbf{u}_1 & \ldots & \mathbf{u}_i & \ldots & \mathbf{u}_m \\ \mathbf{b}_1 \times \mathbf{u}_1 & \ldots & \mathbf{b}_i \times \mathbf{u}_i & \ldots & \mathbf{b}_m \times \mathbf{u}_m \end{bmatrix} \tag{2}$$

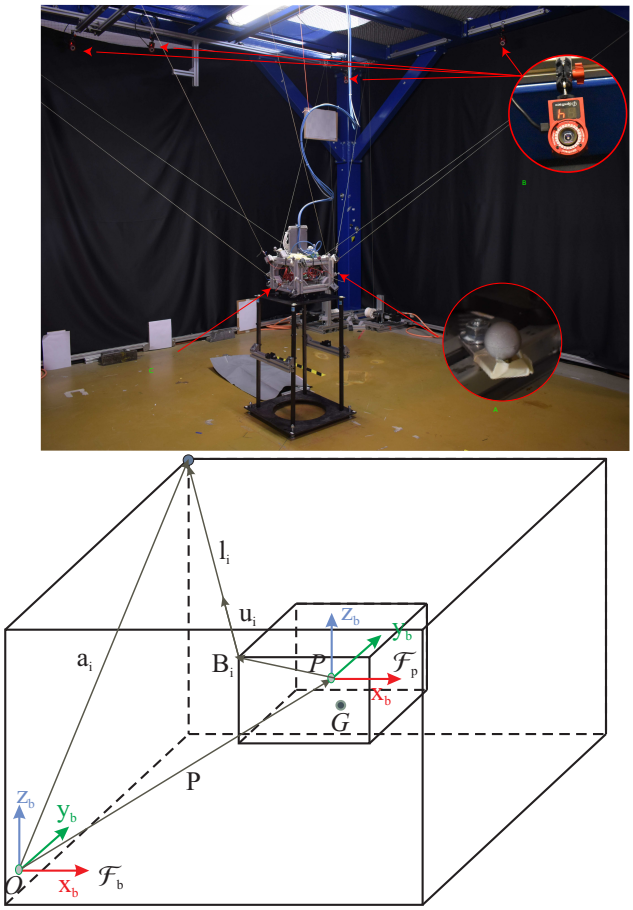

Fig. 1 (left) *CRAFT* prototype located at LS2N, Nantes, France and (right) *CRAFT* Geometric Parametrization.

where $\mathbf{u}_i$ is the unit vector of the i^{th} cable vector pointing from cable anchor points B_i to exit points A_i, expressed in the reference frame $\mathcal{F}_b$. Vector $\mathbf{b}_i$ pointing from point P to point B_i and is expressed in the platform frame $\mathcal{F}_p$. From Eq. (1), $\boldsymbol{\tau} = [\tau_1, \ldots, \tau_i, \ldots, \tau_m]$ is the cable tension vector, $\mathbb{I}_p$ is the inertia tensor, $\mathbf{C}$ is the Coriolis matrix and $\mathbf{w}_g$ is the gravity wrench. $\dot{\mathbf{p}} = \left[\dot{\mathbf{t}}, \boldsymbol{\omega}\right]^\top$ and $\ddot{\mathbf{p}} = \left[\ddot{\mathbf{t}}, \boldsymbol{\alpha}\right]^\top$ are the vectors of the *MP* velocity and acceleration, where, $\dot{\mathbf{t}} = \left[\dot{t}_x, \dot{t}_y, \dot{t}_z\right]^\top$ and $\ddot{\mathbf{t}} = \left[\ddot{t}_x, \ddot{t}_y, \ddot{t}_z\right]^\top$ are the vectors of the *MP* linear velocity and acceleration, while $\boldsymbol{\omega} = \left[\omega_x, \omega_y, \omega_z\right]^\top$ and $\boldsymbol{\alpha} = \left[\alpha_x, \alpha_y, \alpha_z\right]^\top$ are the vectors of the *MP* angular velocity and angular acceleration, respectively. The gravity wrench is:

$$\mathbf{w}_g = m \begin{bmatrix} \mathbf{I}_3 \\ {}^b\mathbf{R}_p\hat{\mathbf{S}}_G \end{bmatrix} \mathbf{g} \tag{3}$$

where m is the *MP* mass, $\mathbf{I}_3$ is the 3×3 identity matrix, ${}^b\mathbf{R}_p$ is the rotation matrix of the *MP* $\mathcal{F}_p$ frame w.r.t the base frame $\mathcal{F}_b$, $\hat{\mathbf{S}}_G$ is the skew-symmetric matrix associated to $\mathbf{s}_G = [x_G, y_G, z_G]^\top$ which represents the coordinate vector of the center of mass of the *MP* expressed in $\mathcal{F}_p$ as:

$$\hat{\mathbf{S}}_G = \begin{bmatrix} 0 & -z_G & y_G \\ z_G & 0 & -x_G \\ -y_G & x_G & 0 \end{bmatrix} \tag{4}$$

$m\,{}^b\mathbf{R}_p\hat{\mathbf{S}}_G$ represents the first momentum of the *MP* defined with respect to base frame $\mathcal{F}_b$. $\mathbf{g} = [0, 0, -g]$ is the gravity acceleration vector where $g = 9.81$ m s^{-2}. The matrix $\mathbb{I}_p$ in Eq. (1) can be

expressed as:

$$\mathbb{I}_p = \begin{bmatrix} m\,\mathbf{I}_3 & -m\,{}^b\mathbf{R}_p\,\hat{\mathbf{S}}_G \\ m\,{}^b\mathbf{R}_p\,\hat{\mathbf{S}}_G & \mathbf{I}_p \end{bmatrix} \tag{5}$$

with $\mathbf{I}_p$ being the MP inertia tensor expressed in $\mathscr{F}_p$. The term $\mathbf{C}$, which represents the centrifugal and Coriolis effects in Eq. (1) is expressed as:

$$\mathbf{C} = \begin{bmatrix} \mathbf{0}_3 & -m\,\hat{\boldsymbol{\omega}}\,\hat{\mathbf{S}}_G \\ \mathbf{0}_3 & \hat{\boldsymbol{\omega}}\,\mathbf{I}_p \end{bmatrix} \tag{6}$$

Using Eqs. (3), (5), and (6) in Eq. (1), gives:

$$\begin{bmatrix} m\,\mathbf{I}_3 & -m\,{}^b\mathbf{R}_p\,\hat{\mathbf{S}}_G \\ m\,{}^b\mathbf{R}_p\,\hat{\mathbf{S}}_G & \mathbf{I}_p \end{bmatrix} \begin{bmatrix} \ddot{\mathbf{t}} \\ \boldsymbol{\alpha} \end{bmatrix} + \begin{bmatrix} \mathbf{0}_3 & -m\,\hat{\boldsymbol{\omega}}\,\hat{\mathbf{S}}_G \\ \mathbf{0}_3 & \hat{\boldsymbol{\omega}}\,\mathbf{I}_p \end{bmatrix} \begin{bmatrix} \dot{\mathbf{t}} \\ \boldsymbol{\omega} \end{bmatrix} - m \begin{bmatrix} \mathbf{I}_3 \\ {}^b\mathbf{R}_p\hat{\mathbf{S}}_G \end{bmatrix} = \mathbf{W}\boldsymbol{\tau} \tag{7}$$

As a first step of the identification, in this article, we will only consider platform translations, *i.e.,* the platform does not rotate in relation to itself. Hence, the angular velocities and accelerations of the MP in Eq. (7) vanish and is reduced to:

$$\begin{bmatrix} m\,\mathbf{I}_3 \\ m\,{}^b\mathbf{R}_p\,\hat{\mathbf{S}}_G \end{bmatrix} [\ddot{\mathbf{t}}] - \begin{bmatrix} m\mathbf{I}_3 \\ m^b\mathbf{R}_p\hat{\mathbf{S}}_G \end{bmatrix} \mathbf{g} = \mathbf{W}\boldsymbol{\tau} \tag{8}$$

As the platform orientation is always constant, we can consider ${}^b\mathbf{R}_p = \mathbf{I}_3$. Eq. (8) can be expressed as in the form as:

$$\mathbf{A}\mathbf{x} = \mathbf{b} \tag{9}$$

where,

$$\mathbf{A} = \begin{bmatrix} \ddot{t}_x & 0 & 0 & 0 \\ \ddot{t}_y & 0 & 0 & 0 \\ \ddot{t}_z + g & 0 & 0 & 0 \\ 0 & 0 & \ddot{t}_z + g & -\ddot{t}_y \\ 0 & -\ddot{t}_z - g & 0 & \ddot{t}_x \\ 0 & \ddot{t}_y & -\ddot{t}_x & 0 \end{bmatrix}, \quad \mathbf{x} = \begin{bmatrix} m \\ mx_G \\ my_G \\ mz_G \end{bmatrix}, \mathbf{b} = \mathbf{W}\boldsymbol{\tau} \tag{10}$$

In Eq. (10), we need the linear acceleration of the MP $\ddot{\mathbf{t}}$ and the cable tensions $\boldsymbol{\tau}$. As the robot is already equipped with the cable tension sensors so we can directly acquire $\boldsymbol{\tau}$.

4 Identification Methodology

The identification methodology is based on the used of the inverse dynamic model (*ID*) Eq. (9), [7], [13], and [9]. This model is linear as function of the four parameters m, mx_G, my_G, and mz_G. An off-line identification of these parameters is then considered, given measured or estimated off-line data for the linear acceleration $\ddot{\mathbf{t}}$ of the MP and the cable tensions $\boldsymbol{\tau}$, collected while the robot *CRAFT* is tracking a planned trajectory. The model Eq. (9) is sampled at a sufficient number of time samples t_i, for $i = 1, \cdots, n_e$, with $(6n_e) \gg 4$, in order to get an over-determined linear system of $(6n_e)$ equations [9]:

$$\mathcal{Y}_{ID}(\boldsymbol{\tau}) = \mathcal{W}_{ID}\mathbf{x} + \rho \tag{11}$$

where

$$\mathcal{Y}_{ID}(\boldsymbol{\tau}) = \begin{pmatrix} b_1(6\times 1) \\ \vdots \\ b_{n_e}(6\times 1) \end{pmatrix} \quad ; \quad \mathcal{W}_{ID} = \begin{pmatrix} A_1(6\times 4) \\ \vdots \\ A_{n_e}(6\times 4) \end{pmatrix}, \tag{12}$$

ρ is the $(6n_e \times 1)$ vector of errors between the data of the experimental measurement of the torques in $\mathcal{Y}_{ID}(6n_e \times 1)$ and the data $\mathcal{W}_{ID}(6n_e \times 4)$ predicted by the model. These errors are due to noise measurement and modeling error. The identification problem consists in finding $\mathbf{x}$ the norm squared of the error ρ:

$$\|\rho\|^2 = \|\mathcal{Y}_{ID} - \mathcal{W}_{ID}\mathbf{x}\|^2 \tag{13}$$

The *LS* estimator models a process by fitting the parameter vector $\mathbf{x}$ according to the minimisation of Eq. (13). Then model (11) becomes

$$\mathcal{Y}_{ID}(\boldsymbol{\tau}) = \mathcal{W}_{ID}\widehat{\mathbf{x}} + \widehat{\rho} \tag{14}$$

The estimated parameter $\widehat{x}$ is equal to:

$$\widehat{\mathbf{x}} = \mathcal{W}_{ID}^{+}\mathcal{Y}_{ID} \tag{15}$$

where $\mathcal{W}_{ID}^{+}$ is the pseudo-inverse of $\mathcal{W}_{ID}$. Since $6n_e > 4$ then $\mathcal{W}_{ID}^{+} = (\mathcal{W}_{ID}^{\top}\mathcal{W}_{ID})^{-1}\mathcal{W}_{ID}^{\top}$. $\widehat{\mathbf{x}}$ is the unique *LS* solution of Eq. (15). The standard deviation $\sigma_{\widehat{\mathbf{x}}}$ is estimated assuming that $\mathcal{W}_{ID}$ is a deterministic matrix and ρ is a zero-mean additive independent Gaussian noise, with a covariance matrix $C_{\rho\rho}$

$$C_{\rho\rho} = E(\rho\rho^{\top}) = \sigma_{\rho}^2\mathbf{I} \tag{16}$$

E is the expectation operator and $\mathbf{I}(6n_e \times 6n_e)$ is the identity matrix. By replacing $\mathcal{Y}_{ID}$ in Eq. (15) with its definition Eq. (11) we obtain:

$$\widehat{\mathbf{x}} = \mathbf{x} + \mathcal{W}_{ID}^{+}\rho \tag{17}$$

Applying the expectation operator at both sides of Eq. (17) ρ being a zero-mean additive independent Gaussian noise we get:

$$E(\widehat{\mathbf{x}}) = E(\mathbf{x}) \tag{18}$$

Thus the estimated values are unbiased. An unbiased estimation of the standard deviation σ_ρ is:

$$\widehat{\sigma}_{\rho}^2 = \frac{\|\mathcal{Y}_{ID} - \mathcal{W}_{ID}\widehat{\mathbf{x}}\|^2}{(6n_e - 4)} \tag{19}$$

$\mathcal{W}_{ID}$ and ρ, being respectively a non-stochastic matrix and a stochastic matrix, the covariance matrix of the *LS* estimation error is then given by:

$$\begin{aligned} C_{\widehat{\mathbf{x}}\widehat{\mathbf{x}}} &= E((\mathbf{x} - \widehat{\mathbf{x}})(\mathbf{x} - \widehat{\mathbf{x}})^{\top}) \\ &= (\mathcal{W}_{ID}^{\top}\mathcal{W}_{ID})^{-1}\mathcal{W}_{ID}^{\top}\,\sigma_{\rho}^2\mathbf{I}\,\mathcal{W}_{ID}(\mathcal{W}_{ID}^{\top}\mathcal{W}_{ID})^{-1} \\ &= \widehat{\sigma}_{\rho}^2(\mathcal{W}_{ID}^{\top}\mathcal{W}_{ID})^{-1} \end{aligned} \tag{20}$$

$\widehat{\sigma}_{\mathbf{x_i}}^2 = C_{\widehat{\mathbf{x}}\widehat{\mathbf{x}}}(i,i)$ is the i^{th} diagonal coefficient of $C_{\widehat{\mathbf{x}}\widehat{\mathbf{x}}}$. The relative standard deviation $\%\widehat{\sigma}_{\mathbf{x_i}}$ for each identified parameters is given by:

$$\%\widehat{\sigma}_{\mathbf{x_i}} = \frac{\widehat{\sigma}_{\mathbf{x_i}}}{|\widehat{x}_i|} \tag{21}$$

The calculation of Eq. (11) and the condition number of $\mathcal{W}_{ID}$ can be obtained using the singular value decomposition (SVD) of $\mathcal{W}_{ID}$.

5 yannick:mono Semi-implicit Homogeneous differentiator

where u is the control input and p a perturbation. Both are considered slowly variable with respect to the sampling period δ i.e. $\forall\, t > 0 \quad \text{and} \quad \forall\, \theta \in [0, \delta] \quad u(t+\theta) - u(t) \simeq 0 \quad \text{and} \quad p(t+\theta) - p(t) \simeq 0$. Then, for time periods of the order of δ equations (??) can be rewritten as follows:

$$\begin{aligned} \dot{x}_1 &= x_2 \\ \dot{x}_2 &= x_3 \\ \dot{x}_3 &= 0 \end{aligned} \tag{22}$$

where $x_3 := u + p$.
With respect to (22) and the fact that only x_1 is measured, the following differentiator [? ?] can be used:

$$\begin{aligned} \dot{z}_1 &= z_2 + \lambda_1 \mu \lceil x_1 - z_1 \rfloor^{\alpha} \\ \dot{z}_2 &= z_3 + \lambda_2 \mu^2 \lceil x_1 - z_1 \rfloor^{2\alpha - 1} \\ \dot{z}_3 &= \lambda_3 \mu^3 \lceil x_1 - z_1 \rfloor^{3\alpha - 2} \end{aligned} \tag{23}$$

with the notation $\lceil \bullet \rfloor^{\alpha} = |\bullet|^{\alpha} \mathrm{sgn}(\bullet)$. For the sake of simplicity, we choose $\mu = 1$ for the rest of the analysis.

The exact implicit discretization of (23) is not possible due to the fact that $\lceil \bullet \rfloor^{\beta}$ with $\beta \notin N$ is not infinitely differentiable in $\bullet = 0$. So there exist many solutions to discretize (23) in explicit way [14?] or semi-implicit way [? ? ? ?], in the next subsection, the method given in [?] is recalled.

5.1 Semi-implicit discretization by multi-projector method.

The method proposed in [?] gives:

$$\begin{aligned} z_1^+ &= z_1 + \delta(z_2^+ + \lambda_1 |x_1 - z_1|^{\alpha} \mathcal{N}_1) - E_2 \frac{\delta^2}{2} z_3^+ \\ z_2^+ &= z_2 + \delta(z_3^+ + E_1 \lambda_2 |x_1 - z_1|^{2\alpha - 1} \mathcal{N}_2) \\ z_3^+ &= z_3 + E_1 E_2 \delta \lambda_3 |x_1 - z_1|^{3\alpha - 2} \mathcal{N}_3 \end{aligned} \tag{24}$$

where the associated projectors $\mathcal{N}_q$ with $q \in \{1, 2, 3\}$ and $\alpha \in [\frac{2}{3}, 1[$ are defined by:

$$\mathcal{N}_q := \begin{cases} \text{if } |e_1|^{q(1-\alpha)} < \lambda_q \delta^q & \rightarrow \mathcal{N}_q = \dfrac{\lceil e_1 \rfloor^{q(1-\alpha)}}{\lambda_q h^q} \\ \text{if } |e_1|^{q(1-\alpha)} \geq \lambda_q \delta^q & \rightarrow \mathcal{N}_q = \mathrm{sgn}(e_1) \end{cases} \tag{25}$$

Moreover, E_i is defined for $i = \{1, 2, 3\}$ such as:

$$E_i := \begin{cases} \text{if } |e_1|^{i(1-\alpha)} < \lambda_i \delta^i & \rightarrow E_i = 1 \\ \text{if } |e_1|^{i(1-\alpha)} \geq \lambda_i \delta^i & \rightarrow E_i^+ = 0 \end{cases} \tag{26}$$

For sufficiently small $\delta > 0$ and an appropriate choice of λ_i $i \in \{1, 2, 3\}$ the differentiator (24) converges exponentially to the solution of (??).

6 Semi-implicit Homogeneous differentiator

The purpose is to estimate the velocity of the angular variable exclusively from the measured position of the output shaft for each of the eight motors. To estimate the angular velocity let us introduce the continuous-time state:

$$\Sigma : \begin{cases} \dot{x}_1 &= x_2 \\ \dot{x}_2 &= p(t) \\ y &= x_1 \end{cases} \tag{27}$$

where x_1 and x_2 are respectively the angular variable and its angular velocity; Here $p(t)$ is a bounded perturbation as it satisfies:

$$\exists p_M > 0 \text{ such that } |p(t)| < p_M \text{ for all } t > 0 \tag{28}$$

y is the measure signal of x_1.$y(t) \in \mathcal{C}^{\bar{\omega}}$ i.e. assumed as an analytic signal:

$$y(t+h) = y(t) + \sum_{j=1}^{\infty} y^{(j)}(t) \frac{h^j}{j!} \tag{29}$$

Homogeneity approach is interesting because if a local stability is obtained due to the dilatation, this framework allows extending this local property to global settings,[15]. This differentiator can be written as [16], [17],

$$\begin{cases} \dot{z}_1 = z_2 + \lambda_1 \mu \lceil \epsilon_1 \rfloor^{\alpha} \\ \dot{z}_2 = \lambda_2 \mu^2 \lceil \epsilon_1 \rfloor^{2\alpha - 1} \\ \hat{y} = z_1 \end{cases} \tag{30}$$

where $\epsilon_1 = y - z_1$; the notation $\lceil \bullet \rfloor^{\alpha} = |\bullet|^{\alpha} \mathrm{sgn}(\bullet)$ is adopted along the paper; $\alpha \in]0.5\ 1[$ has to be fixed [18]. When $\alpha = 1$ the differentiator is linear, $\alpha = 0.5$ defines the proposed differentiator by Levant [19]. This differentiator has the best accuracy with respect to perturbation but it is more sensitive to noise. The choice $\mu^2 > p_M$ is made in order to cancel the effect of the unknown perturbation $p(t)$. λ_i, $i = 1, 2$ are the linear part gains. The homogeneity degree d of the differentiator (30) is equal to $\alpha - 1$ with respect to dilatation Λ_r with $r = (r_1 = 1, r_2 = 1)$ [16]. Moreover, $\lambda_i > 0$, $i = 1, 2$ are the linear part gains, and allow to have the eigenvalues of the differentiation error ϵ_1 in the left part of the complex plane *i.e.* the eigenvalues have a negative real part, while the coefficient μ is chosen sufficiently large to cancel the effect of the unknown perturbation $p(t)$.

The perturbation $p(t)$ is unknown and assumed to be a constant parameter or a slowly variable. This implies that for a sufficient small sampling-time $h > 0$, $p \equiv p^+$, with the notation for a discretized variable:

$$\begin{aligned} \bullet(t = (k+1)h) &= \bullet^+ \\ \bullet(t = kh) &= \bullet. \end{aligned} \tag{31}$$

The implicit Euler discretization of the continuous-time model (27) can therefore be written with (31)

$$\begin{cases} x_1^+ = x_1 + h x_2^+ \\ x_2^+ = x_2 + h p^+ \\ y = x_1 \end{cases} . \tag{32}$$

The discretization of the differentiator Eq. (30) is based on the so-called implicit projection that acts as corrective terms and aim to "generalize" the sign function in sliding-based differentiator in order to reduce the chattering and preserve stability properties for high time steps. Two projectors $\mathcal{N}_1$ and $\mathcal{N}_2$ are used respectively to design the correction terms with the differentiator SIHD-2. In [20], it has been highlighted that the SIHD-2 algorithm offers better performances than with only one projector since the projectors $\mathcal{N}_1$

and $\mathcal{N}_2$ are respectively dedicated to the estimation of z_1 and z_2. Considering the signal to differentiate y, the error $\epsilon_1 = y - z_1$, and the definition of the notation $\lceil \epsilon_1 \rfloor \equiv |\epsilon_1|^{\text{sign}(\epsilon_1)}$, An iterative projector, denoted $\mathcal{N}_q$, where q is the index of differentiation, controls the estimation of each state z_1, z_2 and z_3. The semi-implicit homogeneous Euler discretization based on three projectors (SIHD-3) reads as:

$$\begin{cases} z_3^+ = z_3 + E_1^+ E_2^+ h \left(\lambda_3 \mu^3 \, |e_1|^{3\,\alpha-2} \, \mathcal{N}_3 \right) \\ z_2^+ = z_2 + E_1^+ h \left(z_3^+ + \lambda_2 \mu^2 \, |e_1|^{2\,\alpha-1} \, \mathcal{N}_2 \right) \\ z_1^+ = z_1 + h \left(z_2^+ + \lambda_1 \mu |e_1|^{\alpha} \mathcal{N}_1 \right) \end{cases} \tag{33}$$

where each line z_q^+ is associated respectively to the estimation of the position ($q = 1$), the estimation of the velocity ($q = 1$) and the estimation of the acceleration ($q = 2$). The projector $\mathcal{N}_q$ with $q = 1..3$ is defined:

$$\mathcal{N}_q(\epsilon_1) := \begin{cases} \epsilon_1 \in SD \quad \rightarrow \mathcal{N}_q = \dfrac{\lceil \epsilon_1 \rfloor^{q(1-\alpha)}}{\lambda_q (\mu h)^q}, \quad E_q^+ = 1 \\ \epsilon_1 \notin SD \quad \rightarrow \mathcal{N}_q = \text{sign}(\epsilon_1), \quad E_q^+ = 0, \end{cases} \tag{34}$$

where $SD' = \{\epsilon_1 \in SD / |\epsilon_1| \leq (\lambda_1 \mu^2 h^2)^{\frac{1}{2(1-\alpha)}} \equiv |\epsilon_2| \leq (\lambda_1 \mu^2)^{\frac{1}{2(1-\alpha)}} h^{\frac{\alpha}{1-\alpha}}\}$. The variable E_q^+ allows activating the corresponding $(q+1)$th line when the convergence domain has been reached at the qth line. This prevent from getting unexpected behavior between lines like oscillations that could destabilize the differentiator.

The filtering properties of the differentiator avoid using an extra filter before the differentiation, ~~and the differentiation in two steps offers the possibility of adjusting the homogeneous parameter α with some flexibility.~~ The measured angular positions are noisy such as y becomes $y_m = x_1 + \eta$. The λ_i, $i = 1, 2$ parameters are chosen such as the linear part is stable. The value of homogeneous exponent α is chosen to allow better filtering properties of the estimated differentiation. The μ parameter is also chosen by numerical test trial and error in order to determine the best possible action of the two projectors $\mathcal{N}_1$ and $\mathcal{N}_2$.

7 Experiments

The platform performs four orbital movements. A video of these movements is available at [2]. A sampling period of 10 ms is used to measure the position vector $\mathbf{t}$ and the cable tension $\boldsymbol{\tau}$ with the *FUTEK FSH04097* sensors. Measurement data are recorded over 52 seconds. The eight measured cable tensions are plotted Fig. 3 a). The Euler angles of the platform during its motion are shown in Fig. 3 b). The variations of these Euler angles are small, of the order of 10^{-4} rad. This motion of the platform is indeed translational as it is predicted by the trajectory planning. The identification of the parameters m, mx_G, my_G, and mz_G needs the linear acceleration vector $\ddot{\mathbf{t}}$ of the *MP*. For the best knowledge of this acceleration vector $\ddot{\mathbf{t}}$ a comparison is made from the measured platform position $\mathbf{t}$ between the estimation of the velocity vector $\dot{\mathbf{t}}$ and the acceleration vector $\ddot{\mathbf{t}}$ respectively thanks to the proposed SIHD-2 algorithm and the estimation of these vectors thanks the simplest Euler differentiation method. The estimation of the velocity vector $\dot{\mathbf{t}}$ and the acceleration vector $\ddot{\mathbf{t}}$ with the SIHD-2 differentiator is carried out following two SIHD-2 algorithms is connected in cascade, see Fig. 2. Six parameters are defined for the SIHD-2 algorithm in cascade: λ_1 and λ_2 for the differentiator 1, λ_3 and λ_4 for the differentiator 2, α, and μ. The numerical values of these six parameters are tuned as follows:

$$\begin{aligned} &\lambda_1 = 210, \quad \lambda_2 = 210, \quad \lambda_3 = 525, \\ &\lambda_4 = 525 \quad \alpha = 0.95, \quad \mu = 1. \end{aligned} \tag{35}$$

With the simplest Euler differentiation algorithm the numerical tests shows that the estimation of $\dot{\mathbf{t}}$ and $\ddot{\mathbf{t}}$ requires filtering the position vector $\mathbf{t}$ of the platform with a cutoff frequency of 4Hz. The filter applies a zero-phase forward and reverse digital infinite impulse response (*IIR*) filtering. Figure 4 shows the estimated velocity and acceleration vectors in 3D by using the SIHD-2 algorithm and the simplest Euler differentiation algorithm. The curves are similar between the two algorithms. Table 1 gathers the four identified parameters. The standard deviations are not computed based on the standard deviation from the actual parameter values that are unknown. The numerical values obtained by the two methods for each identified parameter are very close to each other. However, having to filter the position measurement of the platform is a strong constraint in the perspective of doing real time identification of the dynamic parameters of *CRAFT*. That is why the SIDH -2 algorithm, which is iterative, is a relevant solution in the perspective of real time identification.

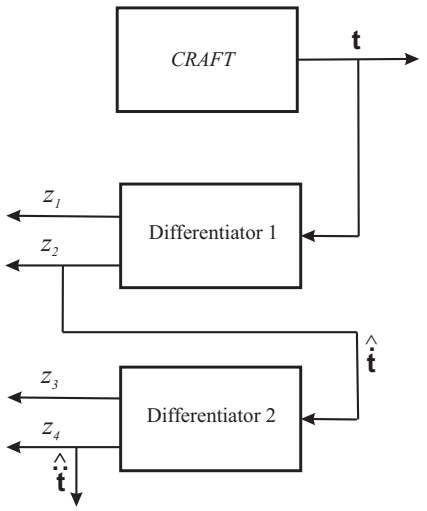

Fig. 2 Estimation variables $\hat{\dot{\mathbf{t}}}$ and $\hat{\ddot{\mathbf{t}}}$ respectively of the linear velocity vector and the linear acceleration vector thanks to the SIHD-2 algorithm with a cascade connection

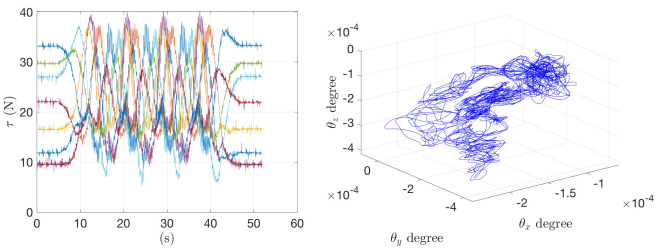

Fig. 3 a) Cable tensions τ as function of time, b) Orientation of the mobile platform.

8 Discussion and Future Work

This research paper presents a novel methodology for identifying the dynamic parameters of Cable-Driven Parallel Robots (CDPRs).

[2] https://youtube/I-IOcAGha3o

Table 1 Numerical values of the identified parameters

Identified parameters	differentiation SIHD-2			Euler differentiation		
	$\widehat{\mathbf{x_i}}$	$\widehat{\sigma_{\mathbf{x_i}}}$	$\%\widehat{\sigma}_{\mathbf{x_i}}$	$\widehat{\mathbf{x_i}}$	$\widehat{\sigma_{\mathbf{x_i}}}$	$\%\widehat{\sigma}_{\mathbf{x_i}}$
m (kG)	9.88	0.0027	0.027	9.88	0.0027	0.027
mx_G (kGm)	-0.064	0.0027	4.21	-0.064	0.0027	4.16
my_G (kGm)	0.019	0.0027	13.86	0.019	0.0027	13.65
mz_G (kGm)	-1.059	0.070	6.67	-1.210	0.078	6.41

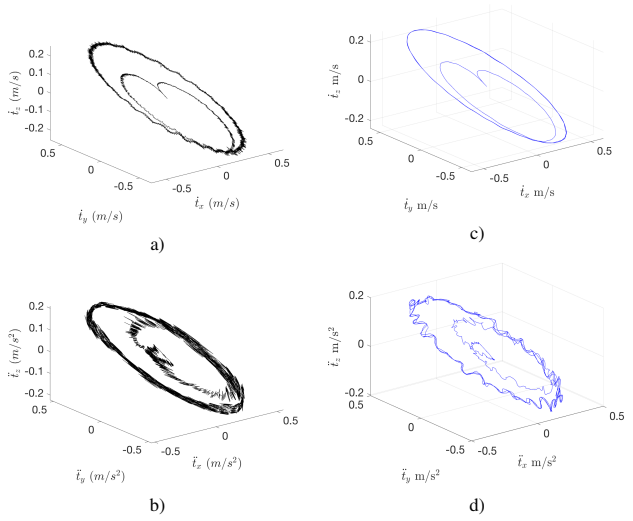

Fig. 4 $\hat{\mathbf{t}}$ and $\dot{\hat{\mathbf{t}}}$ along the orbital trajectory of the platform: velocity (a) and acceleration (b) estimated with the SIDH-2 algorithm; velocity (c) and acceleration (d) computed with the simplest Euler differentiation algorithm.

Initially, the focus is on identifying four parameters, specifically the platform mass and the location of its center of mass, using an orbital trajectory that has been specifically designed to achieve pure platform translation movement in all the three $xyz-$plane. The trajectory, which occurs within a single plane, allows for the identification of these four dynamic parameters. The values determined by the identification of the inertial parameters are consistent with the actual platform mass (measured) and the estimated center of mass location from the computer aided Design. The results have also been compared with other types of trajectories, such as point-to-point linear trajectories. The reason for choosing a circular trajectory is the availability of continuous platform accelerations which facilitates the use of the proposed methodology. The results obtained from experimental measurements of the platform position, as well as measurements treated with the application of a homogeneous semi-implicit differentiator, indicates that despite the complexity of the *CRAFT*. These results allow the real time identification of all the essential dynamic parameters.

In future work, the proposed approach will be used to identify the remaining six dynamic terms associated with the inertia tensor, specifically three terms associated with the platform moment of inertia and other three are products of inertia. To manage the future identification tasks, an IMU sensor will be used in order to provide acceleration measurements that are synchronized with those of the cable tensions. Additionally, we will also aim to identify the friction that acts throughout the actuators of *CRAFT*.

References

[1] Picard, E., Plestan, F., Tahoumi, E., Claveau, F., and Caro, S., 2021, "Control Strategies for a Cable-Driven Parallel Robot with Varying Payload Information," Mechatronics, **79**, p. 102648.

[2] Gouttefarde, M., Collard, J.-F., Riehl, N., and Baradat, C., 2015, "Geometry Selection of a Redundantly Actuated Cable-Suspended Parallel Robot," IEEE Trans. on Robotics, **31**(2), pp. 501–510.

[3] Hussein, H., Santos, J. C., Izard, J.-B., and Gouttefarde, M., 2021, "Smallest Maximum Cable Tension Determination for Cable-Driven Parallel Robots," IEEE Trans. on Robotics, **37**(4), pp. 1186–1205.

[4] Kraus, W., Schmidt, V., Rajendra, P., and Pott, A., 2014, "System identification and cable force control for a cable-driven parallel robot with industrial servo drives," 2014 IEEE Int. Conf. on Robotics and Automation (ICRA), pp. 5921–5926, doi: 10.1109/ICRA.2014.6907731.

[5] Yu, L., Wang, W., Wang, Z., and Wang, L., 2017, "Dynamical model and experimental identification of a cable-driven finger joint for surgical robot," 2017 IEEE Int. Conf. on Mechatronics and Automation (ICMA), pp. 458–463, doi: 10.1109/ICMA.2017.8015860.

[6] Mishra, U. A., Métillon, M., and Caro, S., 2021, "Kinematic Stability based AFG-RRT Path Planning for Cable-Driven Parallel Robots," IEEE Int. Conf. on Robotics and Automation ICRA, Xi'an, China, doi: 10.1109/ICRA48506.2021.9560741.

[7] Gautier, M. and Khalil, W., 1988, "On the identification of the inertial parameters of robots," Proceedings of the 27th IEEE Conf. on Decision and Control, pp. 2264–2269 vol.3, doi: 10.1109/CDC.1988.194738.

[8] Janot, A., Vandanjon, P.-O., and Gautier, M., 2014, "A Generic Instrumental Variable Approach for Industrial Robot Identification," IEEE Trans. on Control Systems Technology, **22**(1), pp. 132–145.

[9] Ardiani, F., 2023, Contribution to the parametric identification of dynamic models: Application to collaborative robotics, Phd Thesis, University of Toulouse, Institut Supérieur de l'Aéronautique et de l'Espace, Toulouse.

[10] Khalil, W. and Dombre, E., 2002, Modeling, identification and control of robots, Butterworth Heinemann.

[11] Michel, L., Selvarajan, S., Ghanes, M., Plestan, F., Aoustin, Y., and Barbot, J. P., 2021, "An experimental investigation of discretized homogeneous differentiators: pneumatic actuator case," IEEE Journal of Emerging and Selected Topics in Industrial Electronics, **2**(3), pp. 227–236.

[12] Michel, L., Ghanes, M., Plestan, F., Aoustin, Y., and Barbot, J.-P., 2021, "Semi-Implicit Homogeneous Euler Differentiator for a Second-Order System: Validation on Real Data," 2021 60th IEEE Conference on Decision and Control (CDC), pp. 5911–5917, doi: 10.1109/CDC45484.2021.9682797.

[13] Gautier, M. and Venture, G., 2013, "Identification of standard dynamic parameters of robots with positive definite inertia matrix," 2013 IEEE/RSJ Int. Conf. on Intelligent Robots and Systems, pp. 5815–5820, doi: 10.1109/IROS.2013.6697198.

[14] Barbot, J.-P., Levant, A., Livne, M., and Lunz, D., 2020, "Discrete differentiators based on sliding modes," Automatica, **112**, p. 108633.

[15] Rosier, L., 1992, "Homogeneous Lyapunov function for homogeneous continuous vector field," Systems & Control Letters, **19**(6), pp. 467–473.

[16] Perruquetti, W., Floquet, T., and Moulay, E., 2008, "Finite-Time Observers: Application to Secure Communication," IEEE Transactions on Automatic Control, **53**(1), pp. 356–360.

[17] Ghanes, M., Barbot, J.-P., Fridman, L., Levant, A., and Boisliveau, R., 2020, "A New Varying-Gain-Exponent-Based Differentiator/Observer: An Efficient Balance Between Linear and Sliding-Mode Algorithms," IEEE Transactions on Automatic Control, **65**(12), pp. 5407–5414.

[18] Hong, Y., Huang, J., and Xu, Y., 2001, "On an output feedback finite-time stabilization problem," IEEE Trans. on Automatic Control, **46**(2), pp. 305–309.

[19] Levant, A., 1993, "Sliding order and sliding accuracy in sliding mode control," Int. J. of control, **58**(6), pp. 1247–1263.

[20] Michel, L., Métillon, M., Caro, S., Ghanes, M., Plestan, F., Barbot, J. P., and Aoustin, Y., 2022, "Experimental validation of two semi-implicit homogeneous discretized differentiators on the CRAFT cable-driven parallel robot," CFM2022, Congrès Français de Mécanique, Nantes, France, https://hal.archives-ouvertes.fr/hal-03751623